Melting of Dense Sodium

Eugene Gregoryanz,[1] Olga Degtyareva,[1] Maddury Somayazulu,[2] Russell J. Hemley,[1] and Ho-kwang Mao[1]
[1]*Geophysical Laboratory, Carnegie Institution of Washington, 5251 Broad Branch Road N.W., Washington D.C. 20015, USA*
[2]*HPCAT, Carnegie Institution of Washington, Advanced Photon Source, Argonne National Laboratory,*
9700 South Cass Avenue, Argonne, Illinois 60439, USA

(Received 26 January 2005; published 13 May 2005)

High-pressure high-temperature synchrotron diffraction measurements reveal a maximum on the melting curve of Na in the bcc phase at ~31 GPa and 1000 K and a steep decrease in melting temperature in its fcc phase. The results extend the melting curve by an order of magnitude up to 130 GPa. Above 103 GPa, Na crystallizes in a sequence of phases with complex structures with unusually low melting temperatures, reaching 300 K at 118 GPa, and an increased melting temperature is observed with further increases in pressure.

DOI: 10.1103/PhysRevLett.94.185502 PACS numbers: 61.10.Nz, 61.20.Ne, 62.50.+p, 64.70.Dv

The alkali group elements are considered textbook examples of free-electron metals because of the single *s* electron in the valence band. However, when these metals are subjected to compression these simple systems exhibit unexpected complexity. Recent theoretical [1,2] and experimental studies [3–6] have shown that this is the case at sufficiently high pressures for dense Li and Na. First-principles calculations predict that Li departs from the free-electron behavior at high densities and its bcc and fcc structures become unstable [1]. Indeed, x-ray diffraction studies have shown that Li undergoes a sequence of phase transitions leading to low-symmetry instead of close packed structures above 40 GPa [3]. The pressure-induced complexity in Li and Na is attributed to the increased role of the core electrons becoming more appreciable with decreased volume [1,2]. Experimental evidence for an increase in resistivity at high pressures and temperatures [7] and the discovery of superconductivity [4–6] in Li showed that the alkali metals are not as simple as they once appeared. With the evidence of a further sequence of phases having complex crystal structures at even higher pressures in Li and Na [3,8] these elements are currently of great theoretical and experimental interest.

Even though the melting temperatures of the alkali metals are relatively low (300–450 K at ambient pressure), their melting curves have been measured over a surprisingly small pressure range, i.e., to 8.0 GPa for Li [9], 11.0 GPa for Na [10], 14.5 GPa for K [10], 14.0 GPa for Rb [11], and 8.0 GPa for Cs [11]. Although high *P*-*T* melting studies have been performed during recent years for a series of elements (see Ref. [12] and references therein), there are certain experimental difficulties that have prevented extensive study of alkali metals. The problems include the difficulty of containing samples at very high *P*-*T* conditions, very high reactivity of the group-I elements, and a lack of unambiguously reliable techniques. Even though experimental data on melting is limited, interesting behavior has been reported for Li where the melting curve appears to flatten, suggesting a maximum around 8–10 GPa [9]; the heavier alkali metals Cs and Rb together with alkaline-earth Ba are reported to exhibit at least two melting curve maxima [13].

Reliable calculations of the melting curves of metals are challenging [14]; however, a thermodynamic perturbation theory study predicted a maximum among the melting curves of the alkali metals [15]. It is accepted that the flattening and bending of the melting curves observed in the heavy alkali and alkali-earth metals [11,13,16], transition metals and other polyvalent metals [17,18] is associated with pressure-induced *s*-*d* band-crossing phenomena. The proposed maxima of the light alkali metals Li and Na do not fit into this explanation, as Li has no *d* bands and Na has a 3*s* conducting band far below the *d* band. This makes the high-pressure behavior of these two elements an important subject of experimental and theoretical study.

In this Letter we report the melting curve of Na measured by x-ray diffraction techniques up to 130 GPa, the highest static pressure at which a melting curve has been measured by external heating techniques. We find a maximum in the melting curve of Na in its bcc phase and a steep decrease of the melting temperature in its fcc phase. We also find that the unusually low melting of the element above 100 GPa is accompanied by the appearance of the new low-symmetry solid phases, along with an increase in the melting temperature above 125 GPa.

We used new high *P*-*T* techniques coupled with synchrotron radiation, an extension of methods employed to study melting curves of hydrogen and oxygen by the means of optical spectroscopy [19,20]. Measurements were carried out using modified high-temperature piston-cylinder Mao-Bell diamond anvil cells equipped with double heaters and thermocouples. Temperature was measured to within ±1 K and ±10 K, respectively, below and above 600 K. Additional details about the heating techniques are provided elsewhere [21]. Experiments were done with Na samples of stated purity of 99.95% (Alfa Aesar), loaded under an Ar atmosphere in a glove box, together with Ta powder for pressure calibration. Diffraction data were collected at beamline 16-ID-B (HPCAT) at the Advanced Photon Source. Focused, monochromatic beams of different wavelengths (0.38–0.42 Å) of the ~15 × 10 μm size were used and the data were recorded during heating on a MAR CCD as well as at room temperature on an image plate calibrated with a Si and/or CeO_2 standard. Pressure was measured using the equation of state of Na [8] and cross-checked with Ta for which P-V-T is known [22] and/or Re/W/Ir which were used as gasket material; for Re, W, Ir we assumed that equation of state is independent of temperature. We conducted 10 separate experiments with pressures ranging from 2 to 130 GPa and temperatures from 275 to 1100 K, the highest temperature apparently reported for the alkali metal in a static pressure experiment.

In the pressure range from ambient to 65 GPa, we observed the bcc phase of sodium. The melting of the bcc Na was evident by the disappearance of bcc reflections and the appearance of diffuse diffraction characteristic of the liquid phase. The discreet steps by which the temperature was changed and the temperature hysteresis which we observed upon melting and solidifying the sample put the error bars of ±70 K on the presented melting temperatures. Figure 1 shows raw images and integrated diffraction data collected in the solid bcc and liquid phases of Na at a pressure of 5.8 GPa. Upon heating, the powder pattern of bcc Na usually transformed into a quasisingle crystal pattern ~100 degrees below actual melting, yielding 3–4 spots visible on a CCD image [Fig. 1(a)]. Reentering the solid phase from liquid by decreasing temperature usually resulted in a decreased number of diffraction spots visible on the image (usually 1–2). The heating/cooling procedure usually led to a complete loss of a diffraction pattern due to the growth of a single crystal of bcc (fcc) Na after three heating cycles, and only diffused scattering was observed rather than a standard diffraction pattern. Change in pressure at 300 K resulted in the reappearance of diffraction spots due to a breakage of the single crystal. In some cases, when the melting temperature was reached, the sample escaped with a loss of pressure and/or breakage of the diamond(s). In that respect, the behavior of hot dense Na resembles that of H_2 at high P-T conditions [19].

Diffraction patterns of the liquid at different pressures are shown in Fig. 2(a). The pressure dependence of $Q = 2\pi/d$ for the first liquid peak of the melted bcc Na was measured up to 62 GPa. The position of the first liquid peak shifts to higher Q, and above 30 GPa, the shift of the diffuse diffraction peak with pressure is slower than the shift of the 110 bcc peak of Na [Fig. 2(b)]. With increasing pressure, the melting temperature of bcc Na first increases, while above 30 GPa it shows a surprising decrease (Fig. 3). According to the Clausius-Clapeyron equation, in the region where the melting curve has a negative slope the liquid is denser than the underlying solid. Some of the P-T paths followed in present study are shown by arrows. The melting curve of bcc Na up to 70 GPa was fit with the Kechin equation [23] giving the maximum of the melting curve at 31 GPa and 1000 K. Note that earlier melting maxima for alkali metals were proposed from the fitting of the measured data with a phenomenological equation [24], that gave a maximum at 38 GPa for Na.

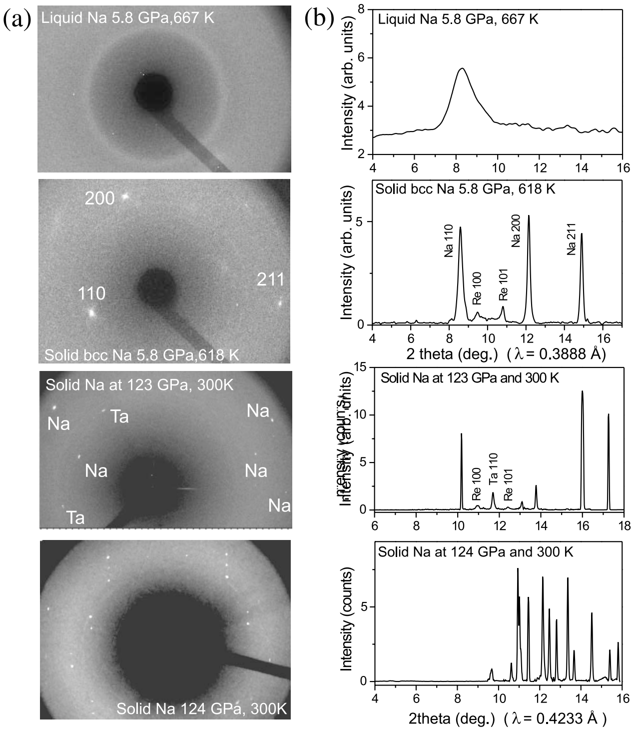

FIG. 1. (a) Diffraction images from liquid and solid phases of Na, collected at 5.8 GPa using synchrotron radiation with wavelength $\lambda = 0.3888$ Å, and at 123 and 124 GPa using $\lambda = 0.4233$ Å. The *hkl* indexing for the bcc diffraction peaks of Na is shown. The peaks of sodium at 123 GPa are marked by "Na"; the spots on the diffraction rings originating from tantalum are marked by "Ta". All diffraction peaks in the 124 GPa image originate from the Na sample. (b) Diffraction patterns from liquid and solid phases of Na at 5.8 GPa, 123 GPa, and 124 GPa, obtained from the integration of the images shown on the left. The diffraction peaks from bcc Na, hcp Re, and bcc Ta are indexed.

On a further pressure increase above 65 GPa at room temperature, we observed the transition from bcc to fcc (see also Ref. [8]). The transition from the solid (fcc) phase to liquid was recorded only by the disappearance of the diffraction reflections from fcc on temperature increase and their reappearance on temperature decrease. No characteristic liquid diffraction was observed, probably due to an insufficient diffraction intensity of a very thin sample. The rapid decrease of the melting temperature of the fcc Na on pressure increase results in the melting temperature of 345 K at 103 GPa, which is lower by ~25 K than the ambient pressure melting point of 370.9 K of bcc Na. We followed the solid fcc pattern at ~675 K on pressure decrease from 80 to 70 GPa (Fig. 3). These measurements combined with the observed melting at lower and higher pressures indicate the existence of a triple point between bcc-fcc solid phases and the liquid at ~65 GPa and 700 K.

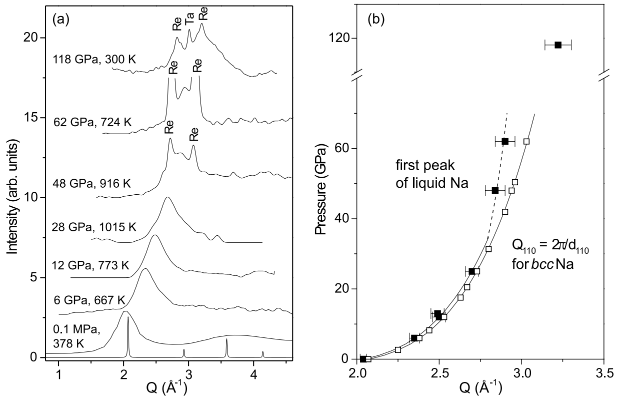

FIG. 2. (a) Diffraction patterns of liquid Na with subtracted background, obtained from different sample loadings at different pressures immediately after melting. The data for liquid Na at ambient pressure are from Ref. [41] and the diffraction pattern of ambient pressure bcc Na is given for comparison. The peaks marked with "Re" are from gasket material; the peak marked "Ta" is from tantalum. (b) pressure dependence of Q of the first diffraction peak of liquid Na (solid symbols) and the 110 diffraction peak of bcc Na (open symbols). The solid lines show the equation of state taken from [8], and the dashed line is a guide to the eye.

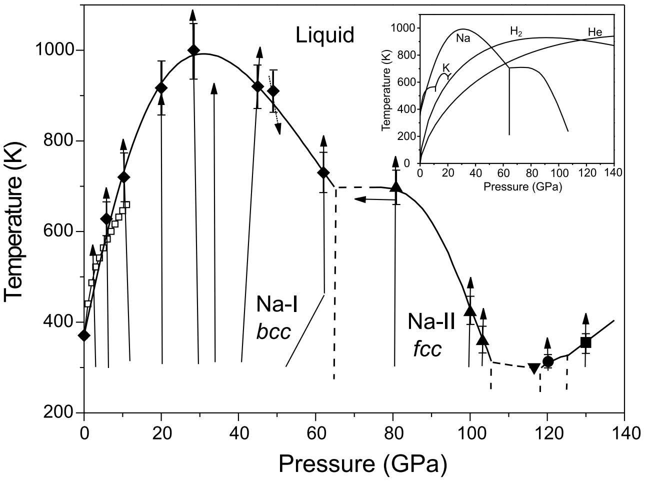

FIG. 3. The melting curve of Na to 130 GPa. The filled symbols are from the present work with different symbols corresponding to the melting of different Na phases. The open squares are from Ref. [10]. The solid line gives the melting curve of bcc Na obtained using the Kechin equation between ambient pressure and 65 GPa; above 65 GPa the solid line is a guide for the eye only (see text). Dashed lines show tentative phase boundaries. The phase relations in the vicinity of the fcc-bcc-liquid triple point are notional. Arrows show various P-T paths followed in the experiments (small pressure shifts on heating are not shown). The inset shows the melting curve of Na (present work) in comparison with the melting curves of H_2 (Ref. [19]) and He (Ref. [30]) and K (Ref. [10]).

Between 103 and 119 GPa at room temperature, Na is reported to form a complex cubic structure with 16 atoms in the unit cell [8], identical to that reported for Li at 40 GPa and 200 K [3]. The disappearance of the diffraction reflections and the appearance of the diffuse diffraction peak [see Fig. 2(a)] at pressure of around 118 GPa and 300 K upon decompression, show that sodium is liquid at room temperature (Fig. 3). Above 119 GPa at 300 K, we observed a sequence of phases with complex diffraction patterns (Fig. 1), indicative of formation of complex crystal structures possibly related to those recently found in the heavier alkali metals [25–27]. A melting temperature as low as 315 K has been measured at 120 GPa, identified by the loss of the reflections from crystalline Na on temperature increase and their reappearance on temperature decrease. Single crystals of the new phases were grown upon cooling, resulting in tens of diffraction spots appearing (see Fig. 1). Upon a further increase in pressure above 125 GPa, we observed an increase in melting temperature (Fig. 3). The resulting phase relation for Na is similar to that reported for Rb [11], Cs [28], and Ba [29]. It appears that for alkali metals the bcc-fcc phase sequence is followed by the transition to the more complex phases which introduces new melting curve behavior.

Although negative melting curves have been reported in some elements and molecular solids, the broad nonmonotonic decrease over a wide pressure range from 35 to above 100 GPa is unique. It is interesting to compare the melting curve of Na with those of He [30] and H_2 [19] which have relatively low melting temperatures (inset in Fig. 3). Hydrogen is of interest because it is expected to dissociate into an atomic simple alkali-like metal at sufficiently high pressures (see Ref. [31] and references therein) possibly having a melting maximum above 100 GPa [19,32] and liquid ground state with unique properties [33].

From the appearance of the melting curve of Na (Fig. 3) different liquid structural and electronic states are expected on the opposite sides of the melting curve maximum. In the region where the melting curve has a negative slope, the molar volume of the liquid is expected to be less than that of the solid. Indeed, different liquids have been reported in molecular systems such as phosphorous [34] where the difference was attributed to the configuration of molecules making up the liquids. For Na a nonmonotonic change in the number of nearest neighbors and interatomic distances in the first coordination sphere is expected. The structure of liquid metals at atmospheric pressure has been described by a hard-sphere-like model which holds under small compression $[(V/V_0)^{1/3} > 0.8]$ [35]. Nevertheless, it was found that for Rb and Cs the deviation from the uniform-compression model happens at $(V/V_0)^{1/3} < 0.85$ [36]. Indeed, very recent studies on the liquid Cs [37] have shown abrupt changes in coordination number and densification. These changes happen in Cs at pressures that correspond to the pressures where the new complex phases in Na appear.

The high-pressure complexity of the crystal structure and melting curve behavior in the heavier alkali metals has been attributed to the effects of s to d transitions in the electronic structures [16,18,38]. However, this cannot apply to the lighter alkali metals such as Li and Na where an *s-p* orbital mixing has been shown for the high-pressure structures [3,39]. The stability of the complex crystal structures in Li, Na, Cs, and Rb [3,25,26] has recently been analyzed within a Hume-Rothery model [40]. It appears that the structural distortions from bcc give rise to new diffraction planes forming a Brillouin zone boundary close to the Fermi surface [40]; interaction between the Brillouin zone boundary and the Fermi surface can then open a pseudogap and reduce the overall band-structure (electronic) energy. This band-structure factor may thus be responsible for the complex behavior of the melting curve of Na.

In conclusion, we have documented unusually low melting temperatures of highly compressed Na. The measurements reveal a sharp decline in the melting temperatures above 30 GPa, arising from major changes in the electronic structure and configurational state of liquid on compression. This first measurement of the negative melting curve in megabar pressure range has implications for the high *P-T* behavior of other putatively simple elemental systems.

We thank N. W. Ashcroft for very useful correspondence and C. Sanloup for stimulating discussions. This work and the use of the HPCAT facility was supported by DOE-BES, DOE-NNSA (CDAC), NSF, DOD-TACOM, and the W. M. Keck Foundation. Use of the Advanced Photon Source was supported by the U.S. Department of Energy, Office of Science, Office of Basic Energy Sciences, under Contract No. W-31-109-Eng-38.

---

[1] J. B. Neaton and N. W. Ashcroft, Nature (London) **400**, 141 (1999).
[2] J. B. Neaton and N. W. Ashcroft, Phys. Rev. Lett., **86**, 2830 (2001).
[3] M. Hanfland, K. Syassen, N. E. Christensen, and D. L. Novikov, Nature (London) **408**, 174 (2000).
[4] K. Shimizu *et al.*, Nature (London) **419**, 597 (2002).
[5] V. V. Struzhkin *et al.*, Science **298**, 1213 (2002).
[6] S. Deemyad and J. S. Schilling, Phys. Rev. Lett., **91**, 167001 (2003).
[7] V. E. Fortov *et al.*, JETP Lett. **70**, 628 (1999).
[8] M. Hanfland, I. Loa, and K. Syassen, Phys. Rev. B **65**, 184109 (2002); K. Syassen, in *High-Pressure Phenomena*, edited by R. J. Hemley, G. Chiarotti, M. Bernasconi, and L. Ulivi (IOS Press, Amsterdam, 2002), p. 251.
[9] H. D. Luedemann and G. C Kennedy, J. Geophys. Res. **73**, 2795 (1968), and references therein.
[10] C.-S. Zha and R. Boehler, Phys. Rev. B **31**, R3199 (1985).
[11] R. Boehler and C.-S. Zha, Physica B (Amsterdam) **139-140B**, 233 (1986).
[12] D. Errandonea, R. Boehler, and M. Ross, Phys. Rev. Lett. **85**, 3444 (2000); R. Boehler, D. Errandonea, and M. Ross, in High-Pressure Phenomena, (Ref. [8]), p. 58.
[13] D. A. Young, *Phase Diagrams of the Elements* (University of California Press, Berkeley, 1991), and references therein.
[14] D. Stroud and N. W. Ashcroft, Phys. Rev. B **5**, 371 (1972).
[15] A. M. Bratkovsky, Phys. Lett. A **130**, 151 (1988).
[16] D. Errandonea, R. Boehler, and M. Ross, Phys. Rev. B **65**, 012108 (2002).
[17] D. Errandonea *et al.*, Phys. Rev. B **63**, 132104 (2001).
[18] M. Ross, L. H. Yang, and R. Boehler, Phys. Rev. B **70**, 184112 (2004).
[19] E. Gregoryanz *et al.*, Phys. Rev. Lett. **90**, 175701 (2003).
[20] M. Santoro, E. Gregoryanz, H. K. Mao, and R. J. Hemley, Phys. Rev. Lett., **93**, 265701 (2004).
[21] E. Gregoryanz *et al.*, Phys. Rev. B **66**, 224108 (2002); E. Gregoryanz *et al.*, *ibid.* **64**, 052103 (2001).
[22] D. Errandonea, M. Somayazulu, D. Hausermann, and H. K. Mao, J. Phys. Condens. Matter **15**, 7635 (2003); A. Dewaele, P. Loubeyre, and M. Mezouar, Phys. Rev. B **69**, 092106 (2004).
[23] V. V. Kechin, Phys. Rev. B **65**, 052102 (2002); J. Phys. Condens. Matter **7**, 531 (1995).
[24] N. Dass, Phys. Rev. B **52**, 3023 (1995).
[25] R. J. Nelmes, M. I. McMahon, J. S. Loveday, and S. Rekhi Phys. Rev. Lett. **88**, 155503 (2002).
[26] M. I. McMahon, R. J. Nelmes, and S. Rekhi, Phys. Rev. Lett. **87**, 255502 (2001).
[27] M. I. McMahon, S. Rekhi, and R. J. Nelmes, Phys. Rev. Lett. **87**, 055501 (2001).
[28] A. Jayaraman, R. C. Newton, and J. M. McDonough, Phys. Rev. **159**, 527 (1967).
[29] M. Winzenick and W. B. Holzapfel, Phys. Rev. B **55**, 101 (1997).
[30] F. Datchi, P. Loubeyre, and R. LeToullec, Phys. Rev. B **61**, 6535 (2000).
[31] H. K. Mao and R. J. Hemley, Rev. Mod. Phys. **66**, 671 (1994); R. Martin, Nature (London) **400**, 117 (1999).
[32] S. Bonev *et al.*, Nature (London) **431**, 669 (2004).
[33] E. Babaev, A. Sudbø, and N. W. Ashcroft, Nature (London) **431**, 666 (2004).
[34] Y. Katayama *et al.*, Nature (London) **403**, 170 (2000).
[35] Y. Waseda, *The Structure of Non-Crystalline Materials*, (McGraw-Hill, New York, 1980).
[36] Y. Katayama and K. Tsuji, J. Phys. Condens. Matter **15**, 6085 (2003).
[37] S. Falconi, L. F. Lundegaard, C. Hejny, and M. I. McMahon, Phys. Rev. Lett. **94**, 125507 (2005).
[38] M. Ross and A. K. McMahan, Phys. Rev. B **26**, 4088 (1982).
[39] N. E. Christensen and D. L. Novikov, Solid State Commun. **119**, 477 (2001).
[40] V. F. Degtyareva, High Press. Res. **23**, 253 (2003).
[41] N. S. Gingrich and L. Heaton, J. Chem. Phys. **34**, 873 (1961).